Circular Polycatenanes: Supramolecular Structures with Topologically Tunable Properties

L. Tubiana[*]
Physics Department, University of Trento, via Sommarive, 14 I-38123 Trento, Italy;
INFN-TIFPA, Trento Institute for Fundamental Physics and Applications, I-38123 Trento, Italy
and Faculty of Physics, University of Vienna, Boltzmanngasse 5, 1090 Vienna, Austria

F. Ferrari
CASA and Institute of Physics, University of Szczecin, Wielkopolska 15, 70-451 Szczecin, Poland*

E. Orlandini
Department of Physics and Astronomy, University of Padova, Via Marzolo 8, I-35131 Padova, Italy
and INFN, Sezione di Padova, Via Marzolo 8, I-35131 Padova, Italy

(Received 18 December 2021; revised 11 August 2022; accepted 4 October 2022; published 23 November 2022)

Polycatenanes, macrochains of topologically interlocked rings with unique physical properties have recently gained considerable interest in supramolecular chemistry, biology, and soft matter. Most of the work has been, so far, focused on linear chains and on their variety of conformational properties compared to standard polymers. Here we go beyond the linear case and show that, by circularizing such macrochains, one can exploit the topology of the local interlockings to store twist in the system, significantly altering its metric and local properties. Moreover, by properly defining the twist (Tw) and writhe (Wr) of these macrorings we show the validity of a relation equivalent to the Călugăreanu-White-Fuller theorem $Tw + Wr = \text{const}$, originally proved for ribbonlike structures such as double stranded DNA. Our results suggest that circular polycatenanes with storable and tunable twist can form a new category of highly designable multiscale structures with potential applications in supramolecular chemistry and material science.

DOI: 10.1103/PhysRevLett.129.227801

Topologically constrained polymers have recently attracted considerable attention in physics, chemistry, and biology [1]. Examples are nanoengineered mechanically interlocked molecules such as rotaxanes, catenanes, and molecular knots [2,3], melts of rings [4], and olympic gels [5–7] such as the natural occurring kinetoplast DNA [8–11]. Steady advancements in chemical synthesis techniques [12–14], modeling, and simulations [15,16] have recently offered a framework to design systems of interlocked rings with controllable properties [13,14,17,18] and versatile applications [19–21]. Examples range from catalyzers and nanomachines [22–26] to candidates for novel smart materials and artificial muscles [27].

Novel experimental techniques allow one to synthesize high-weight polycatenanes, called mechanically interlocked polymers (MIPs), namely long chains composed by n elementary rings held together only by topological interlocking (Hopf links) [13,14,28]. In particular, in Ref. [13] metal supramolecular polymers were used to obtain MIPs composed of up to $n = 130$ rings, while in Ref. [14] a novel self-assembly technique was proposed in which supramolecular rings were grown to form a catenane of up to 22 units [14]. These studies have prompted the question of how the configurational properties of MIPs differ from their standard polymeric counterparts whose elementary units are held together by covalent bonds [29–32].

Interestingly, the possibility of synthesizing cyclic polycatenanes [13] brings up the question of how and to which extent the imposed circular constraint affects the geometry and physics of these structures. For instance, circularized polycatenanes might assume supercoiled configurations as in double stranded DNA (dsDNA), changing their elastic and dynamical properties, and their responsiveness to external stimuli.

Here we show that properly designed circular polycatenanes of semirigid rings [3,13,14] can store a supramolecular twist that affects their equilibrium properties. Since they are geometrically more complex than ribbonlike structures, we provide a strategy to measure the topologically stored twist and extend the notion of twist and writhe of a ribbon to the present context. With this measure we show that by tuning the stored twist and the number of rings n one can control the average extension of the polycatenanes as well as their local properties such as the relative orientation of the rings. Moreover, we provide evidence that a relation equivalent to the Călugăreanu-White-Fuller (CWF) theorem for ribbons [33–37] also holds for circular polycatenanes.

Topological characterization.—From a physical point of view, one can naturally store twist in a circular chain of rings (a circular polycatenane, or "ring-o-rings") by fixing one of the two end rings of an open polycatenane, twisting the other one by a given number of half turns, and linking the two rings to circularize the chain. Each added half turn results in a different topology. These systems are also known as *twisted n-link chains*. In mathematics, physical rings are replaced by unknotted circles so that different topologies can simply be distinguished by including a given integer number of half turns in one circle, while all the others lie in a minimal-twist configuration, e.g., one orthogonal to the next if n is even [38,39]. This elegant approach, however, cannot be applied when dealing with physical rings as the number of half turns is limited by their self-avoidance and rigidity. In the following, we provide an alternative definition suitable for the case of semirigid rings.

Let us consider a circular poly[n]-catenane made of $n = 2k$ planar, oriented rings, whose normals are assigned following the right-hand rule (see also Ref. [39]). For simplicity, we limit ourselves to topologies that admit a planar configuration in which the centers of the rings are placed on the vertices of a regular n-gon on the xy plane, with consecutive rings lying on planes forming alternating angles of $+\delta/2, -\delta/2$ with the xy plane (δ is the angle required to satisfy excluded volume of the rings), and with normals pointing in the $z > 0$ direction; see Fig. 1(a). In this reference configuration (rconf) we can rotate each ring around the catenane backbone so that it lies orthogonally to its immediate neighbors along the chain. This topology coincides with a *minimally twisted n-links chain* [38], and we call it a 0-twist ring-o-rings.

Since the rings are oriented, we can compute the total linking number as $Lk_{\mathrm{tot}} = \sum_{i=1}^{n} Lk_{i,i+1}$, where $Lk_{i,i+1}$ is the linking number between two consecutive rings calculated according to the standard convention for the sign of crossings, and $Lk_{n,n+1} = Lk_{n,1}$ (see Fig. 1 and the Supplemental Material [40]). Clearly $Lk_{\mathrm{tot}} = 0$, as each ring contributes a $+1$ and a -1 link with its neighbors.

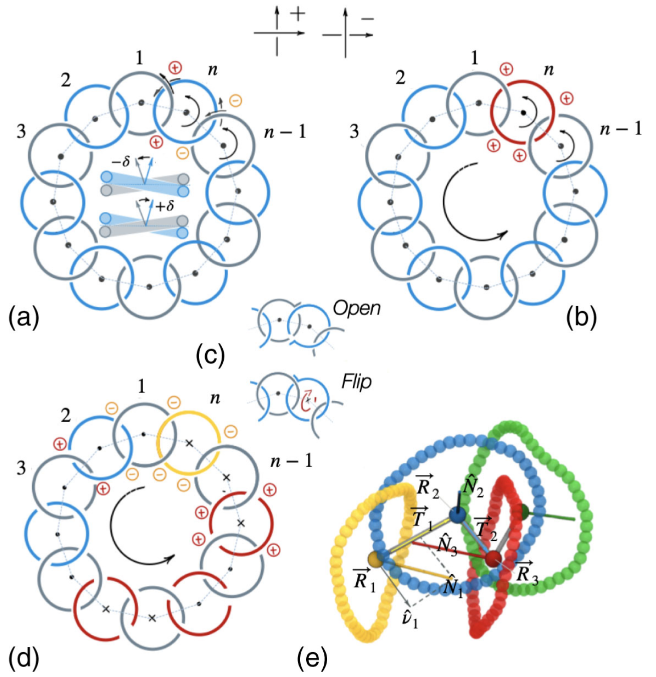

FIG. 1. (a) 0-Twist reference configuration. In the center, we show the twist angles between consecutive normals. The dots inside the rings indicate that all their normals point in the direction $z > 0$. (b) The circular polycatenane resulting from detaching ring n from ring $n - 1$ and closing it switching crossings. (c) The same configuration can be obtained by detaching ring n from ring 1 and flipping it by half a turn before closing the catenane again. The x indicates that the normal of ring n now points below the plane. (d) A circular polycatenane obtained after four clockwise flips of the nth ring, followed by two counterclockwise flips. As explained in the text, all reference configurations can also be obtained by switching the links on even rings, allowing us to calculate the topological invariant $n_{tw} = n_+ - n_-$. The configuration (d) is equivalent to a catenane with $n_+ = 2$ red rings and no yellow rings, as explained in the Supplemental Material [40]. (e) The stiffness of the rings allows us to map them on their centers $\mathbf{R}_i$ and normal vectors $\hat{\mathbf{N}}_i$. Notice how the vectors $\hat{\mathbf{N}}_i$ need not to be perpendicular to the backbone vectors $\mathbf{T}_i$.

Starting from the 0-twist rconf, we construct different topologies by switching the crossings between consecutive pairs of rings in such a way to change the sign of their Hopf links. The total linking number of the catenane can be controlled by focusing on either even or odd rings. Here, we consider the k even rings. Each of them contributes to Lk_{tot} by an amount $Lk_{\mathrm{ring}} \in \{-2, 0, +2\}$ depending on the sign of the Hopf links it forms with its neighbors. In Figs. 1(a)–1(c) these rings are colored in yellow, blue, and red respectively, while odd rings are colored in gray. For instance, in rconf the nth ring is blue and forms a $+1$ Hopf link with ring 1 and a -1 Hopf link with ring $n - 1$. If we detach ring n from $n - 1$ and join them together again in such a way that they form a $+1$ Hopf link, a new configuration rconf′ is obtained with total linking number $Lk_{\mathrm{tot}} = +2$ [see red ring in Fig. 1(b)]. Clearly rconf and rconf′ are topologically inequivalent, because they have different values of Lk_{tot} and the latter is a topological invariant. A yellow ring may be obtained analogously transforming the $+1$ Hopf link made by rings 1 and n into a -1 Hopf link. The resulting new configuration rconf″ has $Lk_{\mathrm{tot}} = -2$.

The change of a ring from blue to red or yellow entails a change of twist. For example, the passage from blue to red can also be implemented by detaching ring n from ring 1, rotating it by an angle $\pi - \delta$ around the backbone, and then rotating ring 1 by an angle δ to link it back to ring n; see Fig. 1(c). If the original orientation of the ring is kept fixed, this operation contributes a $\Delta Tw_0 = \frac{1}{2}$ (half turn) to the initial twist. When defining the normal to point toward

$z > 0$, we obtain $Lk = +2$. Equivalently, transforming a blue ring into a yellow one contributes $\Delta Tw_0 = -\frac{1}{2}$.

Starting from rconf and applying recursively the above procedure on the set of rings $2l$, $l = 1, \ldots, k$, one can store in the system a total initial twist $Tw_0 = \frac{1}{2}(n_+ - n_-)$, where n_+ and n_- are respectively the number of red and yellow rings, ranging in the interval $-k \leq n_{+,-} \leq k$. By making an analogy with Ising systems, one can show that $n_{tw} \equiv n_+ - n_-$ is the only quantity controlling the topology of the system; see the Supplemental Material [40].

Simulated systems.—The polycatenanes are composed of $n = \{20, 40, 60, 80, 100, 200, 300\}$ elementary rings, with $n_{tw}/n = \{0, 0.1, 0.2, 0.3, 0.4, 0.5\}$. Note that this choice of n_{tw} corresponds to Tw_0 being an integer.

Each ring is described by a standard bead-spring model with $m = 48$ beads of diameter σ, giving a thickness-to-diameter ratio $p = \sigma/D = 0.065$; this is compatible with typical polycatenanes obtained from metal-supramolecular polymers [13]. Other values of p, more compatible with either DNA minicircles [3] or supramolecular toroids [14] have been investigated too. The connectivity of each elementary ring is provided by a finitely extensible nonlinear elastic (FENE) potential, and its nominal persistence length is set to $l_p = 2m\sigma$. This level of rigidity prevents substantial variations in local curvature [see Fig. 1(d)], and is compatible with that of the rings used both in Ref. [13] and [14]. Finally, the excluded-volume interaction among the nm beads is treated via a Weeks-Chandler-Andersen potential; see the Supplemental Material [40] for more details.

The systems are evolved starting from their planar configuration using an underdamped Langevin dynamics integrated numerically with the LAMMPS package [41], with default values for the mass, temperature, energy coefficients, and damping time $\tau_d = 10\tau_{LJ}$, where τ_{LJ} is the characteristic simulation time (see the Supplemental Material [40] for more details).

In Fig. 2 we report some typical equilibrium configurations of circular polycatenanes for $n = 20, 300$ and $n_{tw}/n = 0, 0.5$: one can readily see that, for fixed n, configurations with large n_{tw} are more crumpled than untwisted ones ($n_{tw} = 0$). Moreover, as n increases, twisted configurations start to form curled substructures reminiscent of the plectonemes in supercoiled DNA [42]. Although n is not very large, branchedlike structures can be observed for $n = 300$.

Observables.—To characterize the behavior of circular polycatenanes and their relation to closed ribbons, we take advantage of the semirigidity of the rings and coarse grain the systems as follows:

$$\mathbf{R}_i = \frac{1}{m}\sum_{k=1}^{m}\mathbf{r}_k, \qquad \mathbf{T}_i = \mathbf{R}_{i+1} - \mathbf{R}_i, \tag{1}$$

$$\mathbf{N}_i = \frac{4}{3m}\sum_{k=1}^{3m/4}(\mathbf{r}_{k+m/4} - \mathbf{R}_i) \times (\mathbf{r}_k - \mathbf{R}_i), \tag{2}$$

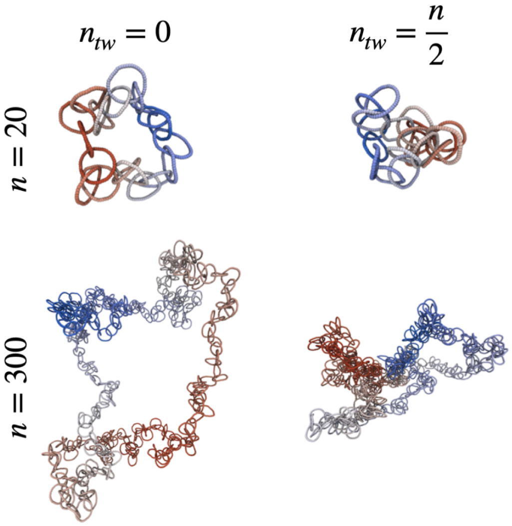

FIG. 2. Typical configurations for $n = 20, 300$ rings with $n_{tw} = 0$ (left column) and $n_{tw} = 0.5n$ (right column). The latter are visibly more crumpled. The scale of the snapshot is preserved at fixed values of n. The color map highlights the sequence of elementary rings along the backbone.

$$\hat{\boldsymbol{\nu}}_k = \frac{\hat{\mathbf{N}}_k - (\hat{\mathbf{N}}_k \cdot \mathbf{T}_k)\mathbf{T}_k}{\|\hat{\mathbf{N}}_k - (\hat{\mathbf{N}}_k \cdot \mathbf{T}_k)\mathbf{T}_k\|} \tag{3}$$

where $\mathbf{r}_k$ is the position of the kth bead on ring i, $\mathbf{R}_i$ is its center of mass, $\mathbf{T}_i$ the bond vector, $\hat{\mathbf{N}}_i = \mathbf{N}_i/|\mathbf{N}_i|$ the normal of ring i, and $\hat{\boldsymbol{\nu}}_i$ is the normalized component of $\hat{\mathbf{N}}_i$ orthogonal to $\tilde{\mathbf{T}}_i$; see Fig. 1(e). Keeping the analogy with twisted ribbons, the beads are numbered so that in rconf all normals points up in the 0-Twist ring-o-rings, while each time a red ring is introduced, its normal and those of successive rings are reversed to follow an equivalent ribbon which is twisted by half turn for each added red ring, so that $Tw_0 = (n_{tw}/2)$.

We first look at the correlation of the ring-ring orientations, $C_n(d, n_{tw}/n) = \langle (1/n) \sum_{i=1}^{n} |\hat{\mathbf{N}}_i \cdot \hat{\mathbf{N}}_{i+d}| \rangle$, where the average is performed over all pairs of rings at distance d taken from all configurations sampled at fixed n_{tw}/n. Note that $C_n(d, n_{tw}/n)$ neither depends on the rings' orientation, nor on the catenane size n. The results are reported in Fig. 3(a) as $\Delta C_n(d, n_{tw}) = C_n(d, n_{tw}/n) - C_n(d, 0)$, normalized by $C_n(d, 0)$, with $C_n(d, 0)$ shown in the inset. For $d \geq 3$, $C_n(d, 0)$ is equal to $1/2$, the average angle between two random planes. $C_n(1, 0) < 1/2$ and $C_n(2, 0) > 1/2$ indicate that when $n_{tw} = 0$ the rings have alternated orientations. Rings' orientation in systems with larger values of n_{tw}/n decorrelate at distances $d \geq 5$, indicating a change in the local arrangement of the rings due to torsion.

To check whether more global observables are affected by the injected twist, we looked at the squared radius of gyration of the backbone, $R_g^2(n, n_{tw})$, computed using the

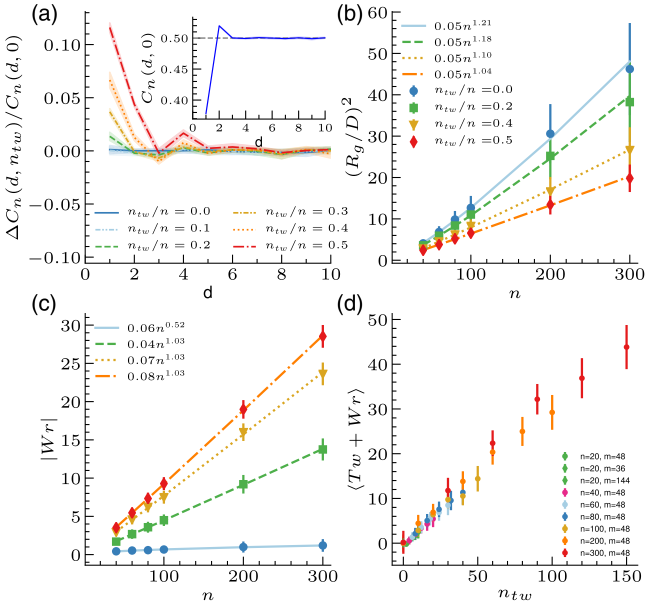

FIG. 3. (a) $\Delta C_n(d, n_{tw}/n)/C_n(d, 0)$ as a function of the index distance d along the backbone, for six different values of n_{tw}/n. (b) Squared radius of gyration as a function of n and n_{tw}/n. R_g is in units of $D = m/\pi$. (c) Scaling of the absolute value of the writhe $|Wr|$ with n, for different values of n_{tw}/n. (d) $\langle Tw + Wr \rangle$ for different values of n_{tw} and n. Results for $n = 20$ include different aspect ratios p. The error bars correspond to the standard deviation of the reported values.

coarse-grained coordinates $\mathbf{R}_i$. All distances were measured in units of the ideal ring diameter $D = m/\pi$. As shown in Fig. 3(b), the stored twist significantly affects the value of $R_g^2(n, n_{tw})$: going from $n_{tw} = 0$ to $n_{tw} = n/2$ at fixed n the polycatenanes become roughly twice as compact. Furthermore, although the simulated systems are not sufficiently long to draw conclusions on the exponent of the expected scaling $R_g^2 \sim An^{2\nu}$, the estimated shapes of the curves in the extreme cases $R_g^2(n, 0)$ and $R_g^2(n, n/2)$ suggest that a sufficiently large initial twist may change the scaling of the gyration radius of the polycatenane from the self avoiding walk class $\nu = 0.587297(7)$ [43] to the branched polymer one with excluded volume $\nu = 0.5$ [44,45]. This crossover has been, for instance, observed in very long and supercoiled dsDNA rings [42] as well as in concentrated solutions of polymer rings [46,47] or rings in the presence of obstacles [48].

The fact that circular polycatenanes take on configurations which resemble supercoiled DNA (see also the snapshots reported in Fig. 2 for $n = 300$) can be further tested by looking at the n dependence of the absolute value of the writhe of the backbone $|Wr|(n, n_{tw})$. The writhe is defined as the number of signed crossings of the backbone averaged over all projections, and captures the amount of coiling of a closed curve on itself [35,36,49,50]. The exact formula is reported in the Supplemental Material [40]. The behavior of $|Wr|(n, n_{tw})$ is reported in Fig. 3(c) for different values of n_{tw}. The difference in the scaling behavior of $|Wr|(n, n_{tw})$ for relaxed and torsionally stressed polycatenanes is evident. For the former case, $|Wr|(n, 0) \sim n^{1/2}$, as expected by rigorous and numerical results on unconstrained random polygons [51,52]. On the other hand, as soon as a finite density of initial twist is trapped along the circular polycatenanes, $|Wr|(n, n_{tw} > 0) \sim B(n_{tw})n$. This transition from the sublinear to linear regime is a genuine feature of circular polycatenanes that cannot be observed in standard models of linear unstructured polymer chains unless they are either strongly confined [53–55] or collapsed into globular shapes by effective attractive interactions [56].

We now test whether the CWF theorem proved for smooth circular ribbonlike structures such as dsDNA rings [33–37] holds in some form for circular polycatenanes. We recall that for a closed ribbon the theorem states that the linking number between its two boundaries satisfies the conservation law $Lk = Tw + Wr$, where Tw is the total twist of the ribbon while the writhe Wr measures the amount of coiling of the ribbon centerline (see the Supplemental Material [40] for more details).

Unfortunately, circular polycatenanes cannot easily be mapped into smooth ribbons, as each of their elementary rings has a significant orientational freedom [see Fig. 3(a)]. Nonetheless, since the rings are sufficiently rigid, we can map the macroring onto a ribbon whose boundaries are given by the curve joining the center of masses $\mathbf{R}_i$ and the curve joining the tips of the vectors $\hat{\boldsymbol{\nu}}_i$ [see Fig. 1(e) and Eq. (3)]. We can thus measure Tw and Wr for circular polycatenanes, and check whether the relation $Tw + Wr =$ constant holds (see the Supplemental Material [40] and Ref. [49] for details).

For each configuration we find indeed that $Tw + Wr \in \mathbb{Z}$. We verified this by taking the fractional part of $Tw + Wr$, and found the relation to hold up to a factor of order 10^{-9}, with a standard deviation of 10^{-12}, compatible with the fact that the rings are not perfectly rigid. Furthermore, we notice that $\langle Tw + Wr \rangle = \alpha n_{tw/2}$ [see Fig. 3(d)], where the factor $\alpha < 1$ comes from the fact that the twist angle between two consecutive normals is defined in $[-\pi, \pi]$, and our coarse graining is equivalent to a piecewise ribbon in which two successive normals can be twisted by an angle larger than $|\pi|$ (see the Supplemental Material [40] for details). This is equivalent to saying that $Tw \bmod(1) + Wr = n_{tw/2}$. The fact that Tw is defined mod(1) is a known aspect of the original Călugăreanu theorem which can be dispensed away for smooth ribbons, but might be present in general [36] (see Ref. [57]).

Finally, we investigate how the configurational properties of circular polycatenanes depend on the thickness-to-diameter ratio, $p = \sigma/D$, of the elementary rings. This has been done for $n = 20$, $n_{tw} = 0$, 10, and $p = 0.022$, 0.065, 0.087. The result $Tw + Wr \in \mathbb{Z}$ holds for all p. Furthermore we notice that, for the range of p values commonly used in self-assembled polycatenanes, the effective compression of the system is apparent and persists over about 1 order of magnitude, with $(Rg/D)^2(n_{tw}/n = 0)$ ranging between 1.52 ± 0.30 for $p = 0.022$ to 1.67 ± 0.33 for $p = 0.087$, while for $n_{tw}/n = 0.5$ $(Rg/D)^2$ is consistently smaller, ranging from 1.05 ± 0.20 for $p = 0.022$ to 1.07 ± 0.16 for $p = 0.087$, giving a a compression factor of about 50% (see the Supplemental Material [40]).

In conclusion, we demonstrated how circularized polycatenanes (ring-o-rings) can store a controllable amount of twist, that radically affects their equilibrium properties. We identified a topological parameter n_{tw} which quantifies the amount of twist initially stored into the system, and showed that it dictates both the relative orientation of nearest-neighbor rings and the scaling of the mean extension R_g and writhe $|Wr|$. Arguably, n_{tw} can be measured experimentally as long as a planar configuration of a polycatenane is available, e.g., by atomic force microscope techniques [60].

Remarkably, our results show that the famous Călugăreanu-White-Fuller relation for dsDNA and ribbons holds also for circular polycatenanes up to a factor mod (1) in the definition of the twist, $Tw \bmod (1) + Wr = \text{const}$, independently of the choice of normals of the elementary rings.

It is worth stressing that the above results remain valid for circular polycatenanes in good solvent conditions and over a wide range of ring thickness-to-diameter ratios, and should be observable experimentally in systems such as double-stranded DNA catenanes [61], synthetic polymeric polycatenanes [13,14], and at much larger scales, macroscopic rings-o-rings in which thermal fluctuations are replaced by randomized mechanical stimuli.

Finally, we believe that the model and findings presented here could be of interest for further developments in supramolecular chemistry and in the physics of soft materials, particularly soft robotics [62,63]. Moreover, as the Călugăreanu-White-Fuller relation links a local geometrical property, the twist, to a global one, the writhe, we believe that circular chains of topologically interlocked rings could inspire future works not only in mathematics and theoretical physics [35,36,64,65] but also, and most prominently, in the field of highly responsive soft self-assembled materials with tunable properties.

This article is based upon work from COST Action CA17139 Eutopia, supported by COST. L. T. acknowledges support from the MIUR grant Rita Levi Montalcini. The research of F. F. and L. T. has been supported in part by the Polish National Science Centre under Grant No. 2020/37/B/ST3/01471. The authors are grateful to R. Ricca and T. Tarenzi for their insight in several useful discussions.

---

[*] luca.tubiana@unitn.it

[1] E. Orlandini and C. Micheletti, Topological and physical links in soft matter systems, J. Phys. Condens. Matter **34**, 013002 (2022).

[2] J. E. Lewis, M. Galli, and S. M. Goldup, Properties and emerging applications of mechanically interlocked ligands, Chem. Commun. **53**, 298 (2017).

[3] X. Liang, L. Li, J. Tang, M. Komiyama, and K. Ariga, Dynamism of supramolecular DNA/RNA nanoarchitectonics: From interlocked structures to molecular machines, Bull. Chem. Soc. Jpn. **93**, 581 (2020).

[4] M. Kapnistos, M. Lang, D. Vlassopoulos, W. Pyckhout-Hintzen, D. Richter, D. Cho, T. Chang, and M. Rubinstein, Unexpected power-law stress relaxation of entangled ring polymers, Nat. Mater. **7**, 997 (2008).

[5] P.-G. De Gennes and P.-G. Gennes, *Scaling Concepts in Polymer Physics* (Cornell University Press, Ithaca, 1979).

[6] J. Fischer, M. Lang, and J.-U. Sommer, The formation and structure of Olympic gels, J. Chem. Phys. **143**, 243114 (2015).

[7] B. A. Krajina, A. Zhu, S. C. Heilshorn, and A. J. Spakowitz, Active DNA Olympic Hydrogels Driven by Topoisomerase Activity, Phys. Rev. Lett. **121**, 148001 (2018).

[8] J. Chen, C. A. Rauch, J. H. White, P. T. Englund, and N. R. Cozzarelli, The topology of the kinetoplast DNA network, Cell **80**, 61 (1995).

[9] A. R. Klotz, B. W. Soh, and P. S. Doyle, Equilibrium structure and deformation response of 2D kinetoplast sheets, Proc. Natl. Acad. Sci. U.S.A. **117**, 121 (2020).

[10] B. W. Soh and P. S. Doyle, Deformation response of catenated DNA networks in a planar elongational field, ACS Macro Lett. **9**, 944 (2020).

[11] J. M. Polson, E. J. Garcia, and A. R. Klotz, Flatness and intrinsic curvature of linked-ring membranes, Soft Matter **17**, 10505 (2021).

[12] Q. Chen, S. C. Bae, and S. Granick, Directed self-assembly of a colloidal kagome lattice, Nature (London) **469**, 381 (2011).

[13] Q. Wu, P. M. Rauscher, X. Lang, R. J. Wojtecki, J. J. De Pablo, M. J. Hore, and S. J. Rowan, Poly [n] catenanes: Synthesis of molecular interlocked chains, Science **358**, 1434 (2017).

[14] S. Datta, Y. Kato, S. Higashiharaguchi, K. Aratsu, A. Isobe, T. Saito, D. D. Prabhu, Y. Kitamoto, M. J. Hollamby, A. J. Smith *et al.*, Self-assembled poly-catenanes from supramolecular toroidal building blocks, Nature (London) **583**, 400 (2020).

[15] M. Marenda, E. Orlandini, and C. Micheletti, Discovering privileged topologies of molecular knots with self-assembling models, Nat. Commun. **9**, 3051 (2018).

[16] M. A. Ubertini and A. Rosa, Computer simulations of melts of ring polymers with nonconserved topology: A dynamic Monte Carlo lattice model, Phys. Rev. E **104**, 054503 (2021).

[17] A. Livoreil, C. O. Dietrich-Buchecker, and J.-P. Sauvage, Electrochemically triggered swinging of a [2]-catenate, J. Am. Chem. Soc. **116**, 9399 (1994).

[18] L. Hu, C.-H. Lu, and I. Willner, Switchable catalytic DNA catenanes, Nano Lett. **15**, 2099 (2015).

[19] V. Aucagne, J. Berná, J. D. Crowley, S. M. Goldup, K. D. Hänni, D. A. Leigh, P. J. Lusby, V. E. Ronaldson, A. M. Slawin, A. Viterisi *et al.*, Catalytic "Active-Metal" Template Synthesis of [2] Rotaxanes,[3] Rotaxanes, and Molecular Shuttles, and Some Observations on the Mechanism of the

Cu (I)-Catalyzed Azide-Alkyne 1, 3-Cycloaddition, J. Am. Chem. Soc. **129**, 11950 (2007).

[20] J.-F. Ayme, J. E. Beves, C. J. Campbell, G. Gil-Ramírez, D. A. Leigh, and A. J. Stephens, Strong and selective anion binding within the central cavity of molecular knots and links, J. Am. Chem. Soc. **137**, 9812 (2015).

[21] Y. Liu, Y. Ma, Y. Zhao, X. Sun, F. Gándara, H. Furukawa, Z. Liu, H. Zhu, C. Zhu, K. Suenaga *et al.*, Weaving of organic threads into a crystalline covalent organic framework, Science **351**, 365 (2016).

[22] T. D. Nguyen, H.-R. Tseng, P. C. Celestre, A. H. Flood, Y. Liu, J. F. Stoddart, and J. I. Zink, A reversible molecular valve, Proc. Natl. Acad. Sci. U.S.A. **102**, 10029 (2005).

[23] D. A. Leigh, J. K. Wong, F. Dehez, and F. Zerbetto, Unidirectional rotation in a mechanically interlocked molecular rotor, Nature (London) **424**, 174 (2003).

[24] J. V. Hernández, E. R. Kay, and D. A. Leigh, A reversible synthetic rotary molecular motor, Science **306**, 1532 (2004).

[25] J.-P. Sauvage, J.-P. Collin, S. Durot, J. Frey, V. Heitz, A. Sour, and C. Tock, From chemical topology to molecular machines, C.R. Chim. **13**, 315 (2010).

[26] S. Erbas-Cakmak, D. A. Leigh, C. T. McTernan, and A. L. Nussbaumer, Artificial molecular machines, Chem. Rev. **115**, 10081 (2015).

[27] J.-P. Sauvage, From chemical topology to molecular machines (Nobel lecture), Angew. Chem., Int. Ed. **56**, 11080 (2017).

[28] S. Mena-Hernando and E. M. Pérez, Mechanically interlocked materials. Rotaxanes and catenanes beyond the small molecule, Chem. Soc. Rev. **48**, 5016 (2019).

[29] P. M. Rauscher, S. J. Rowan, and J. J. de Pablo, Topological effects in isolated poly [n] catenanes: Molecular dynamics simulations and Rouse mode analysis, ACS Macro Lett. **7**, 938 (2018).

[30] P. M. Rauscher, K. S. Schweizer, S. J. Rowan, and J. J. de Pablo, Dynamics of poly [n] catenane melts, J. Chem. Phys. **152**, 214901 (2020).

[31] Z. A. Dehaghani, I. Chubak, C. N. Likos, and M. R. Ejtehadi, Effects of topological constraints on linked ring polymers in solvents of varying quality, Soft Matter **16**, 3029 (2020).

[32] H. Lei, J. Zhang, L. Wang, and G. Zhang, Dimensional and shape properties of a single linear polycatenane: Effect of catenation topology, Polymer **212**, 123160 (2021).

[33] G. Călugăreanu, L'intégrale de Gauss et l'analyse des noeuds tridimensionnels, Rev. Math. Pures Appl **4**, 5 (1959).

[34] F. B. Fuller, Decomposition of the linking number of a closed ribbon: A problem from molecular biology, Proc. Natl. Acad. Sci. U.S.A. **75**, 3557 (1978).

[35] J. H. White, Self-linking and the Gauss integral in higher dimensions, Am. J. Math. **91**, 693 (1969).

[36] H. K. Moffatt and R. L. Ricca, in *Knots and Applications* (World Scientific, Singapore, 1995), pp. 251–269.

[37] R. D. Kamien, The geometry of soft materials: A primer, Rev. Mod. Phys. **74**, 953 (2002).

[38] J. Kaiser, J. S. Purcell, and C. Rollins, Volumes of chain links, J. Knot Theory Ramif. **21**, 1250115 (2012).

[39] The choice of $n = 2k$ does not change the physics of the system. Indeed, one can choose $n = 2k + 1$ and control the position of the even (odd) rings up to $2k$. The extra ring only adds a non-zero minimal twist as described in [38].

[40] See Supplemental Material at http://link.aps.org/supplemental/10.1103/PhysRevLett.129.227801 for detailed description of polymer model, system setup, simulation details and conformational analysis. Proof that n_{tw} is invariant. Additional plots supporting the results.

[41] A. P. Thompson, H. M. Aktulga, R. Berger *et al.*, LAMMPS - a flexible simulation tool for particle-based materials modeling at the atomic, meso, and continuum scales, Comp. Phys. Comm. **271**, 108171 (2022).

[42] B. A. Krajina and A. J. Spakowitz, Large-scale conformational transitions in supercoiled DNA revealed by coarse-grained simulation, Biophys. J. **111**, 1339 (2016).

[43] N. Clisby, Accurate Estimate of the Critical Exponent ν for Self-Avoiding Walks via a Fast Implementation of the Pivot Algorithm, Phys. Rev. Lett. **104**, 055702 (2010).

[44] G. Parisi and N. Sourlas, Critical Behavior of Branched Polymers and the Lee-Yang Edge Singularity, Phys. Rev. Lett. **46**, 871 (1981).

[45] R. Everaers, A. Y. Grosberg, M. Rubinstein, and A. Rosa, Flory theory of randomly branched polymers, Soft Matter **13**, 1223 (2017).

[46] R. D. Schram, A. Rosa, and R. Everaers, Local loop opening in untangled ring polymer melts: A detailed "Feynman test" of models for the large scale structure, Soft Matter **15**, 2418 (2019).

[47] J. D. Halverson, J. Smrek, K. Kremer, and A. Y. Grosberg, From a melt of rings to chromosome territories: The role of topological constraints in genome folding, Rep. Prog. Phys. **77**, 022601 (2014).

[48] A. Khokhlov and S. Nechaev, Polymer chain in an array of obstacles, Phys. Lett. **112A**, 156 (1985).

[49] K. Klenin and J. Langowski, Computation of writhe in modeling of supercoiled DNA, Biopolymers **54**, 307 (2000).

[50] A. D. Bates, A. Maxwell *et al.*, *DNA Topology* (Oxford University Press, USA, 2005).

[51] E. J. van Rensburg, E. Orlandini, D. Sumners, M. Tesi, and S. Whittington, The writhe of a self-avoiding polygon, J. Phys. A **26**, L981 (1993).

[52] J. Portillo, Y. Diao, R. Scharein, J. Arsuaga, and M. Vazquez, On the mean and variance of the writhe of random polygons, J. Phys. A **44**, 275004 (2011).

[53] E. Panagiotou, K. C. Millett, and S. Lambropoulou, The linking number and the writhe of uniform random walks and polygons in confined spaces, J. Phys. A **43**, 045208 (2010).

[54] J. F. Marko, Scaling of linking and writhing numbers for spherically confined and topologically equilibrated flexible polymers, J. Stat. Phys. **142**, 1353 (2011).

[55] C. Micheletti, D. Marenduzzo, E. Orlandini, and D. Summers, Knotting of random ring polymers in confined spaces, J. Chem. Phys. **124**, 064903 (2006).

[56] M. Baiesi, E. Orlandini, and S. G. Whittington, Interplay between writhe and knotting for swollen and compact polymers, J. Chem. Phys. **131**, 154902 (2009).

[57] Indeed, it can be demonstrated that for two pairs of linked curves, A, B, and A', B', one has $Lk(A,B) - Lk(A',B') = \phi(A,A') + \phi(B,B')$, where $\phi(X,X')$ is the integer number of times the curve X winds up around X' [58]. A consistent choice of the two curves, for instance the two

sugar-phosphate backbones in dsDNA, ensures that $\phi(A, A') + \phi(B, B') = 0$, see [59]. In a polycatenane, where no geometrically definite backbone can be identified due to the local freedom of the rings, such a consistent choice is non-trivial. As a consequence, $\phi(A, A') + \phi(B, B') \in \mathbb{Z}$, and thus $Tw + Wr \in \mathbb{Z}$.

[58] J. H. White, in *New Scientific Applications of Geometry and Topology*, edited by L. S. De Witt and N. R. Cozzarelli, Proceedings of Symposia in Applied Mathematics Vol. 45 (American Mathematical Soc., Providence, 1992), p. 17.

[59] N. G. Hunt and J. E. Hearst, Elastic model of DNA supercoiling in the infinite-length limit, J. Chem. Phys. **95**, 9329 (1991).

[60] J. G. Beton, R. Moorehead, L. Helfmann, R. Gray, B. W. Hoogenboom, A. P. Joseph, M. Topf, and A. L. Pyne, TopoStats-a program for automated tracing of biomolecules from AFM images, Methods **193**, 68 (2021).

[61] T. L. Schmidt and A. Heckel, Construction of a structurally defined double-stranded DNA catenane, Nano Lett. **11**, 1739 (2011).

[62] L. M. Castano and A. B. FlatauSmart fabric sensors and e-textile technologies: A review, Smart Mater. Struct. **23**, 053001 (2014).

[63] J. Xiong, J. Chen, and P. S. Lee,Functional fibers and fabrics for soft robotics, wearables, and human-robot interface, Adv. Mater. **33**, 2002640 (2021).

[64] B. Duplantier, Linking numbers, contacts, and mutual inductances of a random set of closed curves, Commun. Math. Phys. **82**, 41 (1981).

[65] M. Dennis and J. Hannay, Geometry of Călugăreanu's theorem, Proc. R. Soc. A **461**, 3245 (2005).